ADVANCED THERAPEUTICS
www.advtherap.com

How Does Temporal and Sequential Delivery of Multiple Growth Factors Affect Vascularization Inside 3D Hydrogels?

*Céline Bastard, Daniel Günther, José Gerardo-Nava, Mieke Dewerchin, Peter Sprycha, Christopher Licht, Arne Lüken, Matthias Wessling, and Laura De Laporte**

Vasculogenesis and angiogenesis are leveraged by orchestrated secretion of several growth factors. Mimicking this process in vitro can maximize vascularization inside 3D cell cultures. While the role of individual growth factors, such as vascular endothelial growth factor, Ephrin-B2, angiopoietins, and platelet-derived growth factor-BB (PDGF-BB) is well studied, the temporal influence of growth factor secretion, and the effect of their concentrations and combinations on in vitro vascularization inside hydrogels, have not been systematically investigated. Here, combinations of angiopoietin-1, angiopoietin-2, and PDGF-BB improve vascularization of a human umbilical vein endothelial cells-fibroblast coculture inside polyethylene glycol-based hydrogels the most, while the optimal concentrations and time points of growth factor addition are determined. Moreover, fibroblasts, pericytes, and mesenchymal stem cells (MSCs) are compared as supporting cells, of which MSCs best promote vascularization in coculture. Additionally, the resulting blood vessels align with magnetically oriented rod-shaped microgels when cultured inside the Anisogel. To mimic fibrosis, transforming growth factor-beta is added, resulting in significantly smaller vessels and more collagen secretion. This in vitro study reveals that a cascade of growth factors can improve vascular formation in 3D hydrogels, which is important to create viable tissue-engineered constructs for therapies and in vitro healthy and diseased tissue models.

1. Introduction

Blood vessel growth has become the holy grail of tissue engineering.[1] Vasculogenesis and angiogenesis require some key features, such as spatial stimuli organization, temporal regulation, cellular crosstalk,[2–4] and active interaction with and remodeling of the extracellular matrix (ECM).[5–8] Without these features, the tightly regulated formation of blood vessels is disrupted.

The natural mechanism of blood vessel formation and maturation relies on the sequential secretion of several growth factors (GFs) at specific concentrations, combinations, and gradients. In the body, the vascular structures need coordinated interactions in time and space between different cell types and multiple GFs to generate a mature network.[6,9–12] Still, the low half-lives and low stability of GFs in the blood flow and inside tissue-engineered scaffolds limit their application in vascular diseases.[13] In addition, adding single GFs to the cell growing in scaffolds usually leads to poorly organized and immature blood vessels.[11] Artificial in vitro systems pose a challenge as GFs have a half-life[13] of maximum 18 h in media, which thus

C. Bastard, D. Günther, J. Gerardo-Nava, P. Sprycha, C. Licht, A. Lüken, M. Wessling, L. De Laporte
DWI – Leibniz-Institute for Interactive Materials
Forckenbeckstr. 50, 52074 Aachen, Germany
E-mail: delaporte@dwi.rwth-aachen.de

C. Bastard, D. Günther, P. Sprycha, C. Licht, L. De Laporte
Institute for Technical and Macromolecular Chemistry
RWTH Aachen University
Worringerweg 1–2, 52074 Aachen, Germany

C. Bastard, D. Günther, J. Gerardo-Nava, L. De Laporte
Institute of Applied Medical Engineering (AME)
Department of Advanced Materials for Biomedicine (AMB)
University Hospital RWTH Aachen
Center for Biohybrid Medical Systems (CMBS)
Forckenbeckstr. 55, 52074 Aachen, Germany

M. Dewerchin, M. Wessling
Laboratory of Angiogenesis and Vascular Metabolism
Center for Cancer Biology (CCB), VIB, and Department of Oncology
KU Leuven
Campus Gasthuisberg ON4, Herestraat 49-902, Leuven 3000, Belgium

A. Lüken, M. Wessling
Chemical Process Engineering
RWTH Aachen University
Forckenbeckstr. 51, 52074 Aachen, Germany

The ORCID identification number(s) for the author(s) of this article can be found under https://doi.org/10.1002/adtp.202300091

DOI: 10.1002/adtp.202300091

requires close monitoring of their activity to ensure their replacement in time.[14]

Multiple GFs have been found to play a role in angiogenesis and vascularization including vascular endothelial growth factor (VEGF), basic fibroblast growth factor (b-FGF), angiopoietin 1 (Ang1), and 2 (Ang2), Ephrin-B2 (Ephr), and platelet-derived growth factor (PDGF). From these, VEGF supports early stages of vascularization, including cell proliferation, migration, and survival, especially VEGF-165 results in the activation of angiogenic signaling pathways.[15,16] In general, several FGFs increase proliferation, survival, stability, and migration. Specifically, b-FGF acts as a mitogen of endothelial cells to stimulate angiogenesis and is further required for the maintenance of endothelial cells and vessel permeability.[17,18] Angiopoietins play an important role in the stabilization and destabilization of the vessel network.[19] While Ang1 appears rather late in the angiogenesis circle and is needed for vascular remodeling,[15] stabilization, and maturation,[20–22] Ang2 works as an antagonist of Ang1 and can, in combination with VEGF, promote vessel sprouting[20] and trigger angiogenesis.[23] Ang1 signals through the tyrosine kinase receptor Tie2 (Tie2), which is endothelial cell-specific. As an antagonist, Ang2 binds with a similar affinity to this receptor as Ang1,[24] blocking the Tie2 receptor from Ang1 and loosening the vascular structures. Sequential exposure to VEGF can then induce new sprouts. The absence of VEGF, however, results in vessel regression and cell death.[20,25–28] In addition, different kinds of ephrins are essential for vascular development.[29,30] For instance, Ephrin-B2 promotes proliferation, sprouting, and motility via endothelial tip cell guidance and adhesion,[31–33] while its pathway is a key regulator for VEGF-mediated angiogenesis.[34,35] If Ephrin-B2 gene expression is disrupted, vein remodeling into properly branched structures is hindered.[29] Finally, PDGF is a factor involved in vascular stabilization, maturation, and remodeling of the vascular wall[36–39] through mural cell guiding, attraction, and interaction with endothelial cells.[40]

Combinations of GFs have demonstrated to have synergistic effects. For example, the combination of Ang1 with VEGF increases the angiogenic sprouting process and enhances the formation of 3D capillary structures.[41] VEGF together with Ang2 promotes endothelial sprouting and enhances microvessel density, while combining them with PDGF and Ang1 inhibits microvessel formation when not temporally controlled. Only when delivered at different time points, this combination can promote vessel maturation and remodeling.[42] These results demonstrate the importance of providing the correct balance of different GFs, their respective temporal addition, and concentrations for successful tissue generation. Since factors can interfere with each other, each factor needs to be selected carefully according to the surrounding conditions.[4]

Therefore, to form complex blood vessels, a perfectly timed sequence of events has to occur with the right cocktail and gradients of biochemical, mechanical, and physical signals, all working together in one big harmonious symphony.[4] When this harmony gets disrupted, several pathologies can occur. For example, transforming growth factor-beta (TGF-β) participates in the pathogenesis of multiple cardiovascular diseases[43] and is a key regulator in tissue fibrosis.[44] It induces the transition process of fibroblasts to myofibroblasts.[45] While a TGF-β blockade diminishes fibrosis,[43] a low concentration (< 0.1 ng mL^{-1}) is cell growth promoting,[46] but a high concentration (10 ng mL^{-1}) induces fibrosis.[47]

To grow blood vessels, different biomaterials can be used as a supporting matrix. Poly(ϵ-caprolactone) (PCL) electrospun fibers are one possibility due to their characteristics of a large surface-to-volume ratio and adjustable porosity. They can be modified with fusion proteins, containing GFs, like VEGF, which enhances cellularization and capillary formation.[48–50] Another possibility is to grow complex blood vessels in 3D hydrogels, as soft water-swollen hydrogels are suitable matrices to mimic the properties of the extracellular matrix (ECM). So far, it was found that specific hydrogels have a high bioactivity and biocompatibility, which makes them attractive candidates for blood vessel growth.[51] The most common ones are fibrin-based hydrogels, due to their fibrous matrix and angiogenesis promoting activity,[52] supporting a high level of network complexity.[53] GFs, like VEGF or basic FGF (b-FGF), can be mixed into fibrin hydrogels and released uncontrollably within 24 h, while in gelatin, alginate, or poly(ethylene glycol) (PEG)-based hydrogels, VEGF or FGF have been bound via heparin, resulting in a slower, local, and more continuous release, which was mainly depending on hydrogel degradation.[54–56] Another possibility is to bind and deliver different angiogenic GFs via engineered GF-binding fibronectin or fibrinogen fragments that are coupled to a fibrin or PEG hydrogel to enhance the proliferation and migration of vascular cells.[57,58]

One limitation of these hydrogel systems is that they are isotropic leading to the formation of randomly oriented blood vessel-like structures, whereas the vasculature in native tissues are hierarchically organized.[59] To introduce cell alignment inside 3D hydrogel, we developed the Anisogel, which consists of magnetically oriented rod-shaped elements embedded inside a surrounding hydrogel.[60–64] So far, these anisotropic hydrogels have been shown to promote aligned growth of fibroblasts and neurites from primary neurons.[60–64]

In this study, we first analyze the individual effect of Ang1, Ephrin-B2, Ang2, and PDGF-BB on the formation of a vascular network inside a polyethylene glycol (PEG)-based hydrogel, modified with fibronectin, as in vitro model, by varying their concentration and timing of delivery. Here, we compare the addition of these growth factors in basal media compared with endothelial growth media, already containing multiple growth factors. We subsequently combine these four growth factors using the most favorable concentrations and time points from the individual studies. Following up on this result, we apply the most successful growth factor cocktail in three exemplary applications: first, with an Anisogel system, targeting the orientation of the formed vessels; second, endothelial cells in combination with other supportive cell types; and third, in a TGF-β-induced fibrosis model.

2. Results and Discussion

2.1. The PEG Hydrogel System to Study Blood Vessel Formation

To study the effect of different growth factors on blood vessel formation inside a 3D in vitro model, we use an enzymatically crosslinked soft PEG-based hydrogel as surrounding 3D matrix.[64,65] Briefly, two peptides, a lysine containing peptide (Ac-FKGGG-PQGIWGQERCG-NH2: K-peptide) that is sensitive to

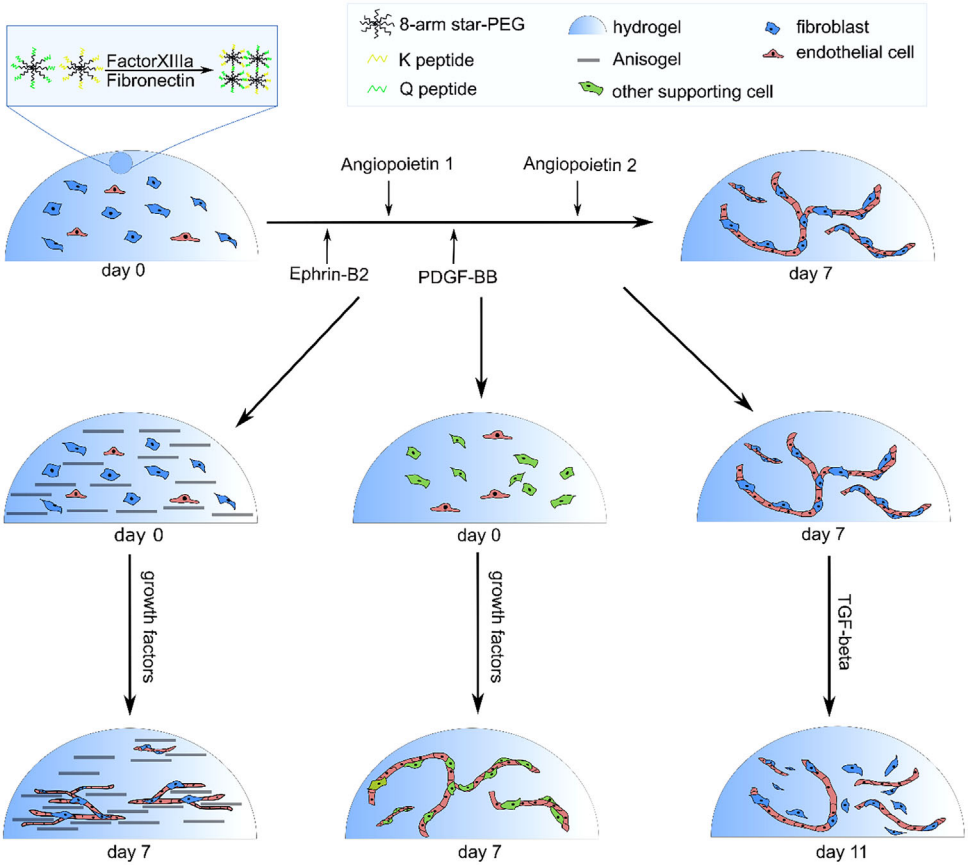

Figure 1. A schematic illustration of the hydrogel system with human umbilical vein endothelial cells (HUVECs, red) and normal human dermal fibroblasts (NHDF, blue) or different supporting cells (green) forming vascular structures. Different growth factors are added to the cocultures in isotropic hydrogels or Anisogels, with or without the addition of TGF-β on day 11 to induce fibrosis.

degradation by matrix metalloproteinases (MMP), produced by cells, and a transglutaminase substrate (H-NQEQVSPLERCG-NH2: Q-peptide), both containing a cysteine, are coupled via a Michael-type addition to an 8-arm star PEG-vinylsulfone (sPEG-VS). The corresponding PEG-K and PEG-Q molecules are mixed in an equimolar ratio at a total of 1–2 wt% in a calcium containing buffer, and the biomolecule fibronectin or fibronectin fragment FN9*–10,12-14, to reach a hydrogel stiffness ranging between 10 and 1350 Pa, unless mentioned otherwise. The mechanical properties of the PEG-hydrogel used in this report have been analyzed before for polymer concentrations ranging from 1 to 5 wt%, demonstrating a storage modulus between 10 and 3800 Pa, respectively.[65] The softest gel resulted in the highest neurite outgrowth[65] and is the most suitable for blood vessel formation (Figure S1, Supporting Information). When human umbilical vein endothelial cells (HUVECs) and fibroblasts are cocultured in a 1, 1.5, or 2 wt% PEG gel, modified with a fibronectin fragment, the branching points of the vascular structures and their total area is the highest in 1 wt% gel (Figure S1, Supporting Information). Therefore, for the remaining studies, the softest gel is selected. Normal human dermal fibroblasts (NHDF) and HUVECs are mixed in a ratio of 3:1 with the PEG-QK precursor solution and endothelial growth media (EGM-2), at a total cell density of 1000 cells μL^{-1} to grow capillary-like structures (**Figure 1**), unless otherwise indicated. The gelation is initiated by the addition of activated Factor XIII and the cells are cultured for 7 days, while multiple growth factors (Table 2) are added at different time points and concentrations in Dulbecco's Modified Eagle's Medium (DMEM), neither basal medium (EBM), or EGM-2 culture media, which already contains GFs, such as VEGF-165, b-FGF, epidermal growth factor (EGF), insulin-like growth factor (IGF), and the other supplements (see the Experimental Section).

2.2. Defining the Optimal Cell Numbers and Ratios to form Vessel Structures

Initially, HUVECs and NHDFs are used to grow vascular structures inside isotropic PEG hydrogels. For cultures using 1000 cells μL^{-1} at an initially tested ratio of HUVECs and NHDFs of 1:1, EBM nor DMEM result in the formation of vascular structures. HUVECs remain as single cells, do not connect with each other (**Figure 2**A,B), and show poor cell proliferation on day 1 (d1) and d3 (Figure S2A,B, Supporting Information). In EGM-2, on the other hand, which already contains GFs like VEGF, cell

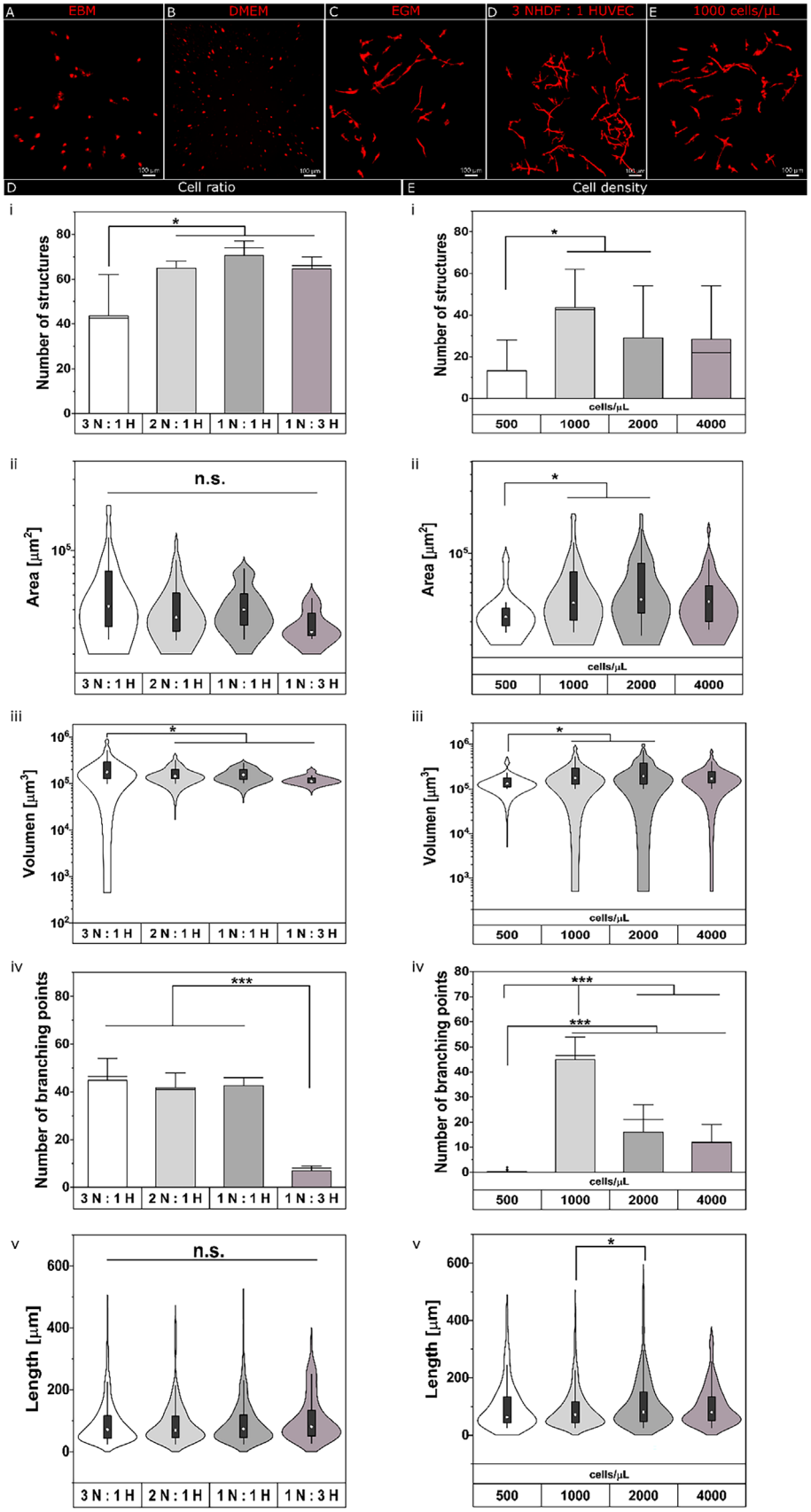

proliferation is higher and HUVECs and NHDFs start to form a vascular-like structure (Figure 2C). This indicates that angiogenic growth factors are required to initiate vessel formation, as previously shown.

To optimize vessel formation, different ratios of NHDFs and HUVECs at 3:1, 2:1, 1:1, or 1:3 are tested (Figure 2D,i-v). While proliferation on d1 and d3 is not affected by the ratio in either type of media (Figure S2A,B, Supporting Information), vascular structure formation, measured by volume ($p < 0.05$) or by area (clear trend but not reaching statistical significance), is clearly improved for 3NHDF:1HUVECs, compared to 1NHDF:1HUVECs, in EGM-2 after 7 days of culture (Figure 2D,i-v). The number of structures is significantly lower for 3NHDF:1HUVEC cultures (≈45) compared to the other three ratios (≈70), which is inherent to having more connected structures and increased total area and volume. The median volume of these structures is indeed significantly higher with values reaching 1.7×10^5 μm^3 for 3NHDF:1HUVEC compared to 1.4–1.1 $\times 10^5$ μm^3 for the other cell ratios. This result is unexpected as other groups reported that higher fractional numbers of HUVECs in such cocultures lead to good vascular structures. For example, in a macroporous sponge-like gel,[66] in a fibrin or fibrinogen-based hydrogel,[53,67] or a hybrid fibrin plus macroporous scaffold,[53] a 5HUVEC:1fibroblast ratio led to a 3D vessel-like network in vitro or in vivo. In contrast, in our hydrogel, a high number of HUVECs compared to NHDFs results in a small reduction in the area and volume of vascular structures but a significantly lower number of branching points, while the total length of the structures is unaffected by these ratios.

To determine the optimal cell density, the 3:1 NHDF: HUVEC ratio is selected and the total cell number is varied from 500 to 4000 cells μL^{-1} in the hydrogel precursor volume (Figure 2E,i-v). A cell density of 500 cells μL^{-1} is too low to form vascular structures as the number of structures, their area, their volume, and the branching points are significantly lower than those found in samples with a cell density of 1000 or 2000 cells μL^{-1}. However, a concentration of 4000 cells μL^{-1} is also inferior to the 1000 or 2000 cells μL^{-1} condition. Possibly, the gels become too crowded leaving no room for higher vascularization, or the gel is rendered unstable, as cells take more space, inhibiting the crosslinking of the gel and reducing its stiffness. Densities of 2000 and 1000 cells μL^{-1} show similar values for area, volume, and length, making the number of branching points the critical deciding parameter. Since a density of 1000 cells μL^{-1} leads to a significantly higher number of branching points of around 45 versus 21 for 2000 cells μL^{-1}, 12 for 4000 cells μL^{-1} or 1 for 500 cells μL^{-1}, this density is chosen for further experiments. This value is also quite low, but it would be in accordance with previous publications, which indicate that around 1×10^6 cells mL^{-1} are required for good vasculature formation.[67,68] A higher cell concentration, therefore, destabilize our gels much faster.

For the further experiments, focused on defining the optimal cocktail of growth factors to promote vascularization, a cell ratio of 3NHDF:1HUVEC, a total cell density of 1000 cells μL^{-1}, and EGM-2 are used as the base to support optimal cell growth.

2.3. Effect of Individual Growth Factors on Vascular Structure Formation

To evaluate the effect of different growth factors on vessel structure formation, the cells are first cultured in EGM-2 until it is replaced with EBM without or with the GF of interest on day 3, 4, 5, or 6. This removes the VEGF, b-FGF, and other factors present in the EGM-2, while the addition of a sequential GF aims at recapitulating the cascade in the body to allow the proper formation of vascular structures.[4,69] The concentrations for Ang1,[41,70] Ephrin-B2,[32,71] PDGF-BB,[40,68,72] and Ang2[73,74] used are based on literature. These doses (Table 2) are chosen supraphysiological since high concentrations are needed to secure diffusion of sufficient GF into the hydrogel. The structures are analyzed after 7 days of culture.

Ang1, a vessel network stabilizer,[20–22] is added on day 3, 4, or 5 at concentrations in the range of 0.2–2 μg mL^{-1} in EBM (**Figure 3**A,i-ii; and Figure S3Ai-iii, Supporting Information). A concentration of 0.7 μg mL^{-1} shows a trend toward higher areas and volumes at all tested time points (d3–d5), with a significantly higher number of branching points (90) on d4 compared to Ang1 concentrations of 0.2, 1.4, and 2 μg mL^{-1}, which led to ≈50 branching points. The number of structures is the lowest when Ang1 is added on d3 without losing area or volume. This suggests more connected structures when Ang1 is added on d3. The number of structures does not significantly alter with Ang1 concentration but when compared to no addition of Ang1, the area and branching points are significantly higher at a concentration of 0.7 μg mL^{-1}. This fits with previous observations that showed that Ang1 leads to larger blood vessels.[12,75]

For PDGF-BB, a factor that remodels and matures the vascular structures,[36] a concentration of 2–40 ng mL^{-1} is added on day 4, 5, or 6 in EBM (Figure 3B,i-ii; and Figure S3B,i-iii, Supporting Information). Here, 40 ng mL^{-1} shows a significant increase in area, volume, and length, especially when added on day 4. If added on d4, the number of branching points is significantly higher with 150 points compared to ≈50–70 for the other concentrations and ≈20 structures when no PDGF-BB is added. Without PDGF-BB, the number of structures is lower compared to all added concentrations at all time points.

Ephrin-B2, which promotes proliferation, sprouting, and motility,[31–33] is added at concentrations of 0.3–2 μg mL^{-1} on days 3, 4, or 5 in EBM (Figure 3C,i-ii; and Figure S3C, i-iii, Supporting Information). More structures are visible when Ephr is added on day 4 and 5 at 0.8 μg mL^{-1} leading to 32 structures compared to 48

Figure 2. Effect of growth media, cell ratios, and cell densities on vascular structure formation in PEG-QK gels. A–C) Immunofluorescence staining for PECAM/CD-31 of structures formed by NHDF:HUVEC cocultures (ratio 1:1) in PEG-VS in EBM A), DMEM B), and EGM-2 C) (red, scale bar: 100 μm). Analysis of number of structures (i), area (ii), volume (iii), branching points (iv), and length (v) for different NHDF:HUVEC cell ratios D) and for different total cell densities E) based on immunofluorescence staining for PECAM/CD-31. NHDF:HUVEC ratios in panel (E) is 3:1. The PEG-VS gels were processed and analyzed after culturing for 7 days in EGM-2. Scale bar: 100 μm. Bar graphs show the range between the first and third quarter indicated by the bar. The outliers and the mean value are represented by the error bars and the horizontal line, respectively. The violin plots show the range between the first and third quarter indicated by the black bar in the violin and its standard deviation by the vertical line. The outliers and median are represented by the violin and the white dot. *n*: 3–6 replicates per condition ($p^* < 0.05$; $p^{**} < 0.01$; $p^{***} < 0.001$).

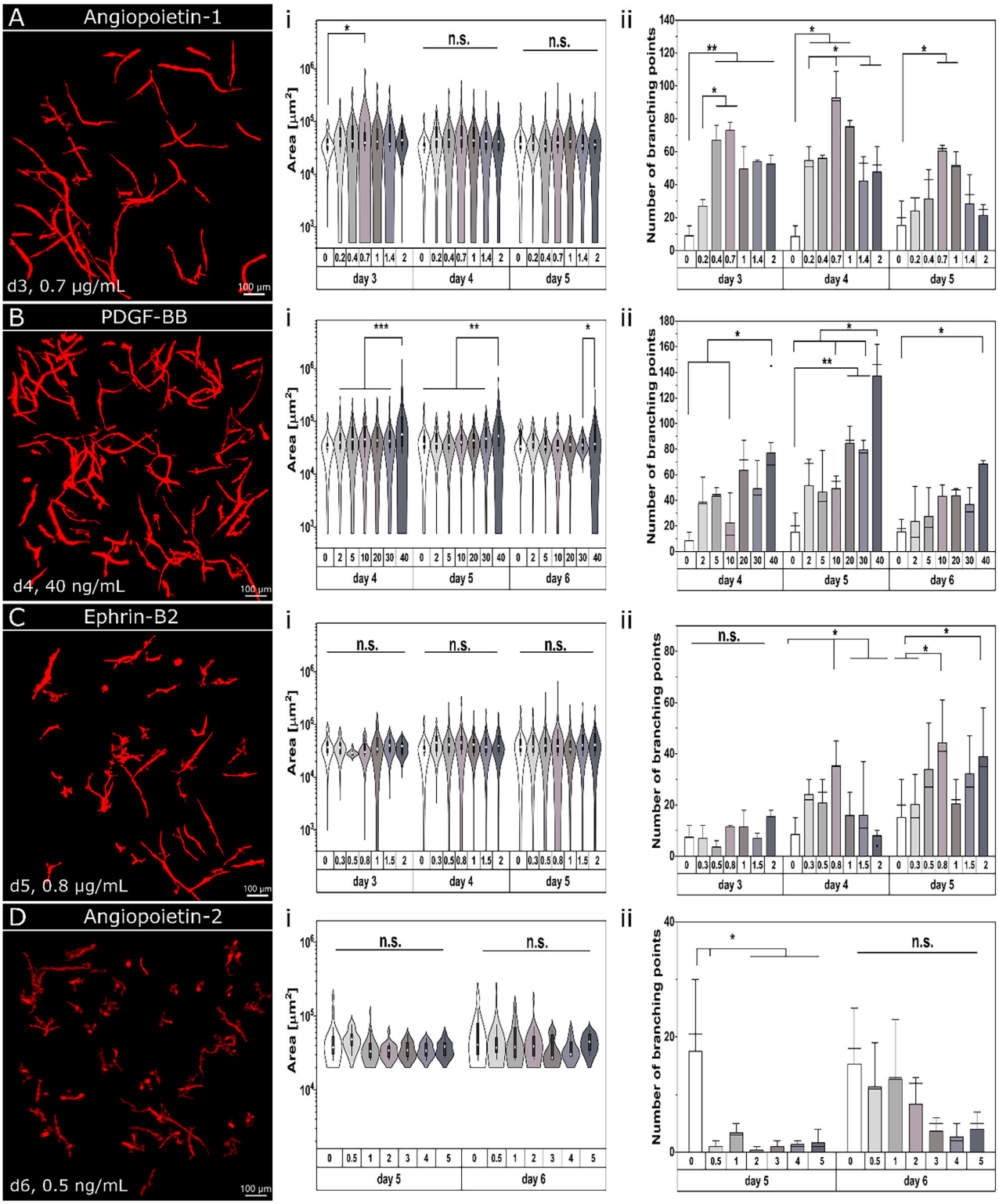

Figure 3. Effect of the individual GFs on vascular growth in PEG-QK gels analyzed after 7 days of culture via immunofluorescence staining of NHDF:HUVEC structures (ratio 3:1) for PECAM/CD-31 (red) grown in EBM, with quantification of the structure area (i) and branching points (ii). Immunostainings show representative images of vascular structures when Ang1 is added on d3 at 0.7 µg mL^{-1} A). PDGF-BB on d4 at 40 ng mL^{-1} B). Ephrin-B2 on d5 at 0.8 µg mL^{-1} C), and Ang2 on d6 at 0.5 ng mL^{-1} D). Scale bar: 100 µm. Bar graphs show the range between the first and third quarter indicated by the bar. The outliers and the mean value are represented by the error bars and the horizontal line, respectively. The violin plots show the range between the first and third quarter indicated by the black bar in the violin and its standard deviation by the vertical line. The outliers and median are represented by the violin and the white dot. $n = 3$–6 replicates per condition ($p^* < 0.05$; $p^{**} < 0.01$; $p^{***} < 0.001$).

in the case of 1 μg mL^{-1} when added on day 4. The timing of Ephr addition and its concentration do not affect the structure area and volume, but a concentration of 0.8 μg mL^{-1} shows a significantly higher number of branching points when Ephr is added on day 4 or 5.

Finally, for Ang2, a key factor in triggering angiogenesis,[23] a concentration of 0.5–5 ng mL^{-1} is added on day 5 or 6 in EBM (Figure 3D,i-ii; and Figure S3D i-iii, Supporting Information). Here, high concentrations of Ang2 lead to smaller structures than low concentrations, with the number of branching points being lower for all Ang2 concentrations (<5 for high concentrations, <10 for low concentrations), compared to the other GFs (20–150). The delivery of Ang2 only, leads to smaller areas and volumes at all concentrations compared to cultures without Ang2, demonstrating that the delivery of Ang2 only has a negative impact on the structures (compared to Figure 2B,C). On d5, the delivery of Ang2 leads also to significantly fewer branching points compared to the EBM control without Ang2. The structure destabilization caused by Ang2 is in agreement with the fact that Ang2, which is added in EBM without VEGF, requires VEGF to stabilize vessel maturation and formation of new sprouts,[20,25,26] an effect was also seen in vivo when the activity of VEGF is inhibited.[76] Therefore, Ang2 will be further tested in combinatorial GF delivery.

Overall, except Ang2, all GFs show a positive effect on the vascular structures with an increase in the area, volume, and branching points. In particular, Ang1 and PDGF lead to significantly more vascular structures in this experimental setup. The addition of Ang2 leads to smaller structures, especially at high concentrations.

2.4. Effect of GFs in Growth Media Containing VEGF, b-FGF, and other Growth Factors

As VEGF is one of the most important GFs and its interaction with Ang2 is well known for the growth of vessels,[20,27] a second screening is performed using individual addition of Ang1, PDGF-BB, Ephrin-B2, and Ang2 in EGM-2. Concentrations and time of addition are done in the same way as in the experiments shown in Figure 3.

Upon addition of Ang1 on d3 or d4, the area and volume of the structures are similar for the different Ang1 concentrations and are larger compared to EGM-2 without Ang1. Even though there are still many small structures (**Figure 4**A,i-ii; and Figure S4A, i-iii, Supporting Information), a concentration of 0.7 μg mL^{-1} Ang1 shows a trend toward structures with the largest area and volume. When added on d5, this concentration also shows significantly more branching points and increased length. Also, on d4, the number of branching points is significantly higher at concentrations 0.7–1 μg mL^{-1} compared to EGM-2 without Ang1. This is in accordance with previous studies, where a concentration of around 0.7 μg mL^{-1} showed a higher number of sprouts, especially in combination with VEGF,[70] making Ang1 a promising candidate for further studies. Based on the above results, to achieve large structures without compromising branching points and length too much, the GF combination experiments following below are performed with 0.7 μg mL^{-1} Ang1 added on day 4.

Next, the effect of the EGM-2 supplemented with PDGF-BB is analyzed (Figure 4B,i-ii; and Figure S4B, i-iii, Supporting Information). Here, the trend is similar to EBM, however, structures are longer and bigger. A PDGF-BB concentration of 40 ng mL^{-1} also shows significantly higher values for area, volume, length, and the number of branching points compared to the other PDGF concentrations in EGM-2. In vivo, a low concentration of PDGF-BB (10 ng mL^{-1}) shows better vascularization but also higher amounts (50 ng mL^{-1}) lead to better results than without PDGF-BB.[72] The number of structures is again not significantly different except when PDFG-BB is added on d5. For all other structure parameters, the best results are observed when PDGF-BB is added on d4. Therefore, this time point is chosen for further experiments using this GF. The addition of PDGF-BB on d4 or d5 is also used in previous publications, but lower concentrations (25 ng mL^{-1}) were sufficient to promote vascular growth,[40] possibly related to the use of other cell types. In this study, HUVECs were cocultured with mesenchymal stem cells (MSCs) and a 2D model was employed instead of 3D.[40]

Upon the addition of Ephrin-B2 in EGM-2, the structures are also longer and bigger compared to its addition in EBM (Figure 4C,i-ii; and Figure S4C i-iii, Supporting Information). This is in agreement with previous research showing that Ephr with VEGF leads to higher endothelial cell proliferation and motility,[31,32] suggesting that more cells make intercellular contact and build larger structures. When Ephr is added on d4 or d5, a higher area and volume are observed for the structures with most structure parameters being optimal at a concentration of 0.8 μg mL^{-1}. This concentration is then chosen, as it promotes significantly more branching points when added on day 4.

Ang2 shows the strongest effect when added together with EGM-2 (Figure 4D,i-ii; and Figure S4D, i-iii, Supporting Information), compared to EBM. When now added on d6, vascular structures show significantly bigger areas and volumes, especially at the lower concentration of 1 ng mL^{-1}. At 1 ng mL^{-1}, the structure volume (3.3×10^5 μm^3) is significantly higher compared to all other concentrations ($1.2–1.8 \times 10^5$ μm^3), confirming the observations in vivo that Ang2 requires VEGF to avoid destabilization of the structures.[76] At higher Ang2 concentrations, the vascular structures fall apart. For in vivo applications, lower GF doses need to be added as high GF concentrations may have negative side effects, like promoting tumor growth. For example, plasma from patients suffering from melanoma cancer shows high Ang2 concentrations (> 4 ng mL^{-1}) outside the range of healthy patients (1–3 ng mL^{-1}), while cell experiments showed that Ang2 can regulate melanoma cell migration and invasion.[73] Here, a concentration of 1 ng mL^{-1} Ang2 is added on d6 for further experiments as it leads to the best formation of vascular structures.

Overall, the combinations of the individual GFs with EGM-2 lead to larger structures, indicating a synergistic action with VEGF-165, b-FGF, EGF, IGF, and/or the other supplements in this medium. Still, there are many small structures present. Therefore, we tested combinations of these four GFs with EGM-2, aiming at further increasing the size and complexity of the structures.

2.5. Combinatorial Delivery of Growth Factors

Since growth factors in vivo are never expressed alone, we tested the four GFs in different combinations in fresh EGM-2 in our in

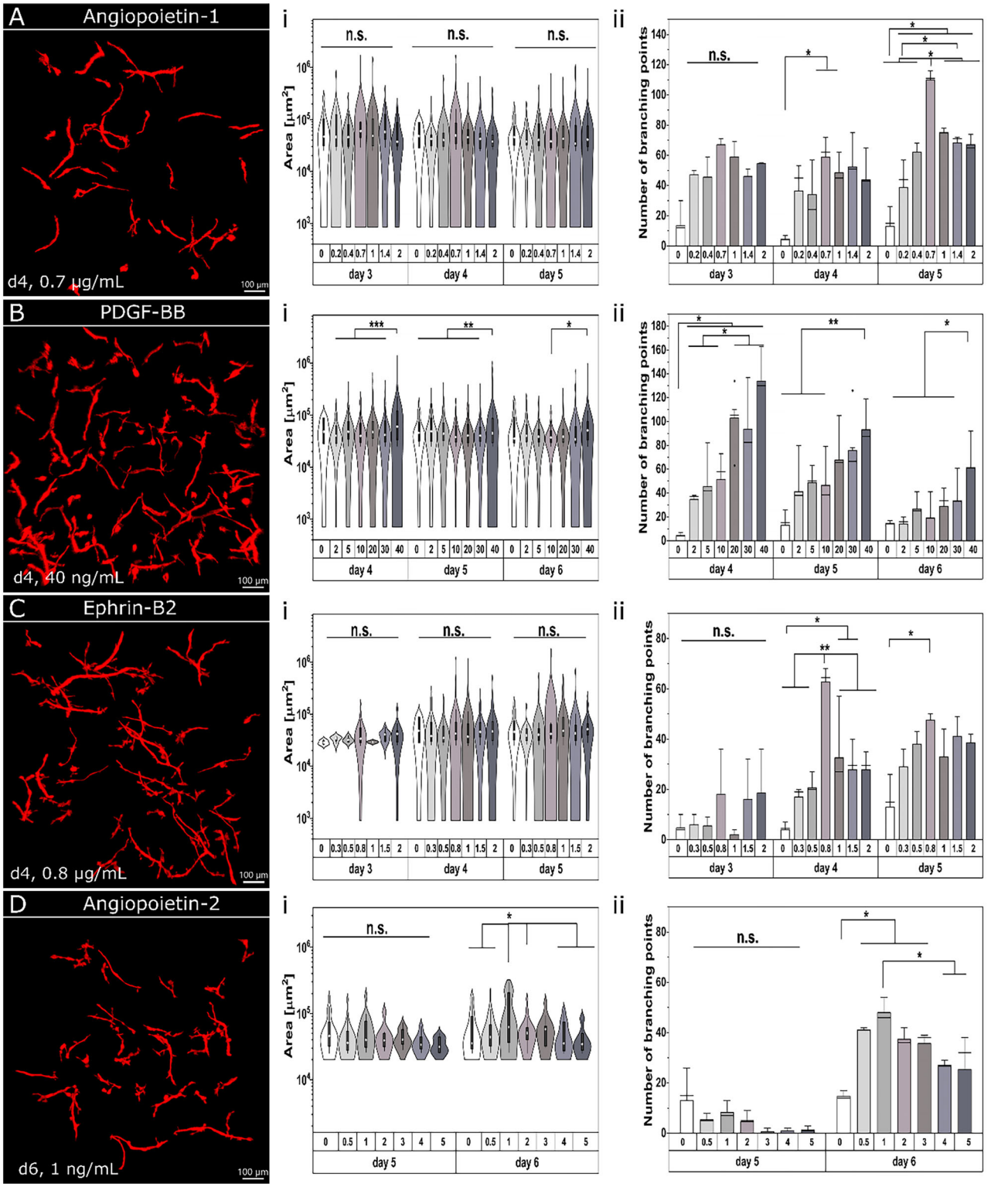

Figure 4. Effect of the individual GFs on vascular growth in PEG-QK gels analyzed after 7 days of culture via immunofluorescence staining of the NHDF:HUVEC structures (ratio 3:1) for PECAM/CD-31 (red,) grown in EGM-2 with quantification of the structure area (i) and branching points (ii). Immunostainings show representative images of vascular structures when Ang1 is added on d4 at 0.7 µg mL^{-1} A). PDGF-BB on d4 at 40 ng mL^{-1} B). Ephr on d4 at 0.8 µg mL^{-1} C). and Ang2 on d6 at 1 ng mL^{-1} D) (scale bar: 100 µm). Bar graphs show the range between the first and third quarter indicated by the bar. The outliers and the mean value are represented by the error bars and the horizontal line, respectively. The violin plots show the range between the first and third quarter indicated by the black bar in the violin and its standard deviation by the vertical line. The outliers and median are represented by the violin and the white dot. $n = 3$–6 replicates per condition ($p^* < 0.05$; $p^{**} < 0.01$; $p^{***} < 0.001$).

Table 1. GF concentration and their application time in the combinatorial GF study.

Growth factor[a)]	Concentrations	Adding day
Ang1	0.7 μg mL^{-1}	day 4
Ephr	0.8 μg mL^{-1}	day 4
PDGF-BB	40 ng mL^{-1}	day 4
Ang2	1 ng mL^{-1}	day 6

[a)] Eleven GF combinations are tested: Ang1+Ephr, Ang1/Ang2, Ephr/Ang2, Ang1+PDGF-BB, PDGF-BB/Ang2, Ephr+PDGF-BB, Ang1+Ephr/Ang2, Ang1+PDGF-BB/Ang2, Ang1+Ephr+PDGF-BB, Ephr+PDGF-BB/Ang2, Ang1+Ephr+PDGF-BB/Ang2.

vitro model by using the concentrations and time points selected during the first screening experiments (**Table 1** and **Figure 5**).

As a control, fresh EGM-2 is added on the same days as the GFs. The results show that the number of structures is the highest when combining Ephr/Ang2 (83 structures), compared to the numbers of structures, ranging between 33 and 57, for all other GF combinations, and compared to GFs added individually with EGM-2. The combinations Ang1/Ang2 and Ang1+Ephr/Ang2, with 55 and 57 structures, respectively, are not statistically significantly lower compared to Ephr/Ang2. Importantly, as mentioned above, fewer structures can be a sign of more connected structures when the area and volume do not decrease. For the area, the combination of Ang1+PDGF/Ang2 is significantly higher than all other combinations, except for Ephr+Ang2. For the structure volume, the same combination is significantly higher than all others. For the number of branching points, also Ang1+PDGF/Ang2 is significantly higher (130) than EGM-2 only (46); Ang1+Ephr (26); Ephr+PDGF (17); Ang1+Ephr+PDGF (23); Ang1+Ephr/Ang2 (56); Ephr+PDGF/Ang2 (26); and to all four GFs combined (36) in EGM. The length values seem similar for most GF combinations, with Ang1+PDGF/Ang2 resulting in a slightly higher overall structure length, while EGM-2 only and Ephr+Ang2 show a significantly lower structure length.

Overall, a combination of Ang1+PDGF/Ang2 in EGM-2 induces the best vascular structure formation and is therefore selected for further investigation inside the Anisogel, to test different supporting cell types, and trigger fibrosis. This combination of growth factors was already tested by Brudno et al.[42] for cells cultured on microcarrier beads and not inside a 3D hydrogel. While recombinant human VEGF (rhVEGF) and Ang2 led to significantly more endothelial cell sprouting, it inhibited microvessel formation when added simultaneously with PDGF-BB/Ang1. Similar to our results, when temporally controlled, i.e., added at different time points, this combination promoted vessel growth and vascular remodeling. Importantly, pericytes were used as supporting cells in combination with HUVECs and the GFs were added daily at different concentrations (50 ng mL^{-1} rhVEGF, 250 ng mL^{-1} Ang2, 50 ng mL^{-1} PDGF-BB, 250 ng mL^{-1} Ang1) for 3 or 5 days.[42]

It is interesting to note that combining all four additional GFs in EGM-2 does not lead to better vascularization, and on the contrary reduces the vessel area and volume. When individually added in EBM, each GF is not affected in its mode of action but when combined with another GF, they can positively or negatively influence each other. To the best of our knowledge, Ang1 and PDGF-BB do not negatively affect each other but show parallel actions,[77] which is also visible in our best GF combination. Therefore, the only GF, which might in combination, negatively affect vascular growth, is Ephrin-B2. It is possible that Ephr, known to induce endothelial cell migration,[31,32] prevented vessel complexity. Ephr is known to inhibit Ang-1 expression, while supporting the expression of Ang-2,[78] removing the positive effects of the added Ang1 when added on the same day. This could explain the smaller area and volume of the vessel structures for all growth factors combined together.

Importantly, to use our optimal growth factor combination (Ang1+PDGF/Ang2) in vivo, novel drug delivery systems have to be developed that enable release at different time points by the design of the material properties and GF-material interactions,[57,79] or by drug delivery systems that can respond to internal or external triggers. For example, sequential delivery of GFs can be achieved by binding or incorporating them into porous polymer scaffolds, while the release rate can be altered by changing the polymer degradation rate[80] or the number of binding sites.[81] In our research group, we have and are still developing hollow microgels that can be loaded with GFs during microfluidic production, which then can be released at different times depending on the shell properties, while the microgels themselves can be mixed inside regenerative hydrogels for in vivo use.[82]

2.6. Endothelial Characterization in the Case of Optimal Growth Factor Combination

After finding the optimal GF combination to grow vascular structures inside the hydrogels, we analyzed markers for endothelial characterization after 7 days of culture. For this, we analyzed the expression of VE-Cadherin, nestin, and factor VIII, as further detailed below.

VE-Cadherin is located at the junction between endothelial cells, critically supports endothelial barrier integrity, and modulates vascular endothelial growth factor receptor functions.[83] VE-cadherin immunostaining signal is visible at the cell–cell junctions of the endothelial cell structures grown inside the hydrogels (**Figure 6**A). This shows that the endothelial cells make contact, and assemble into vascular structures. While Pecam/CD31 is shown in small to large size vessels, nestin, and factor VIII are markers of ongoing angiogenesis.[84] In our work, both markers are detected in the vascular structure with the optimal GF combination (Figure 6B) but more importantly, factor VIII expression is significantly increased in the structures without GFs, while nestin expression is significantly higher in the structures grown in hydrogels with Ang1+PDGF-BB/Ang2 (Figure 6C). This indicates the transition to more complex vessels when our optimal GF combination is added at these time points (d4 and d6).

2.7. Vessel Alignment Inside an Anisogel

As capillaries in the body show some degree of oriented growth, especially when they align with peripheral nerves,[68] the optimal GF cocktail is tested with the HUVEC/fibroblast coculture inside an Anisogel (**Figure 7**). After a brief size screening

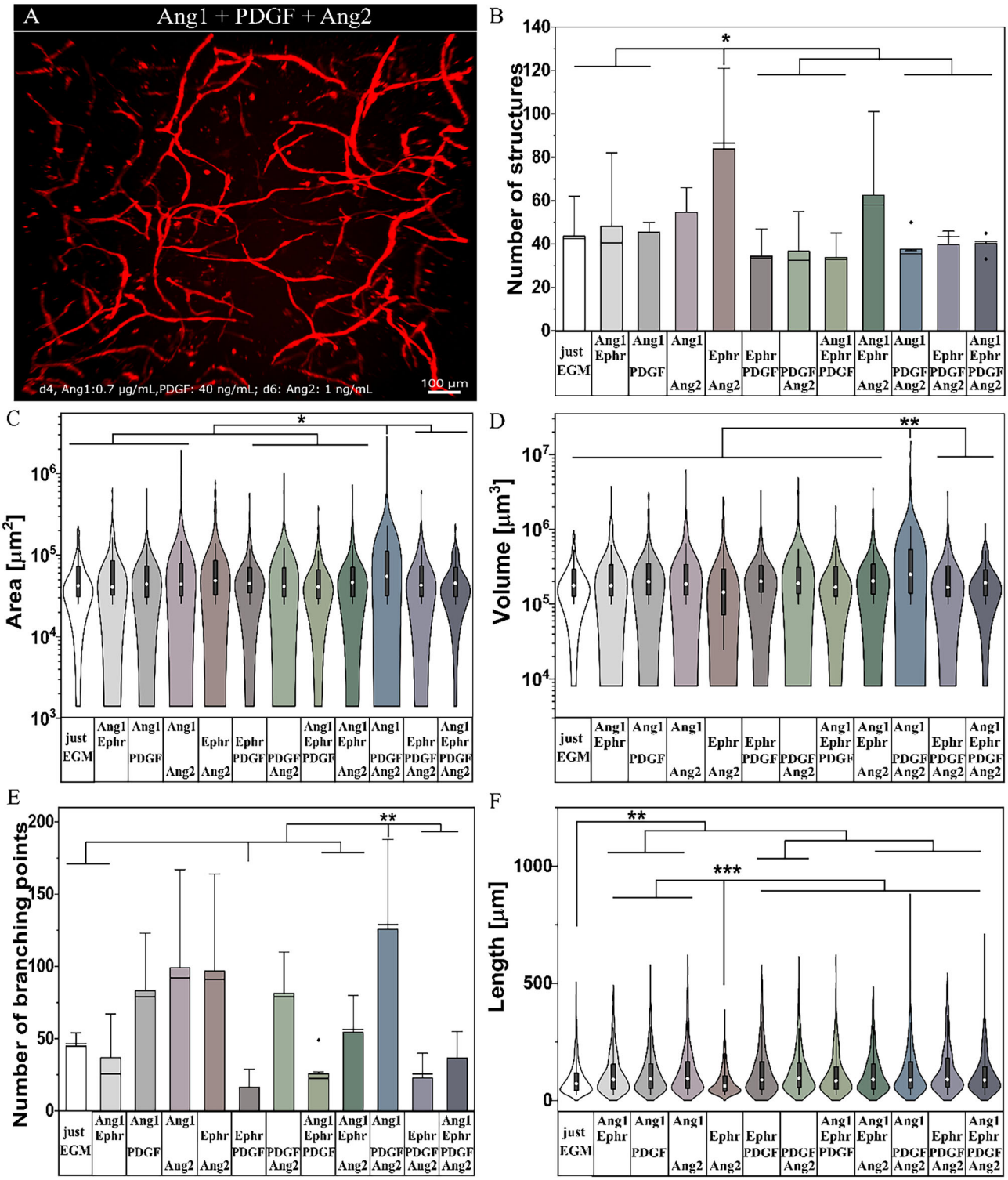

Figure 5. GF combination. A) Immunofluorescence staining of PECAM/CD-31 structure (red) analyzed after 7 days of culture of NHDF:HUVEC mixtures (ratio 3:1) in EGM-2 in the presence of the best GF combination, scale bar: 100 µm; Quantification of structures: number of structures B), area C), volume D), number of branching points E), and length F). Bar graphs show the range between the first and third quarter indicated by the bar. The outliers and the mean value are represented by the error bars and the horizontal line, respectively. The violin plots show the range between the first and third quarter indicated by the black bar in the violin and its standard deviation by the vertical line. The outliers and median are represented by the violin and the white dot. *n*: 6 replicates per condition ($p^* < 0.05$; $p^{**} < 0.01$; $p^{***} < 0.001$).

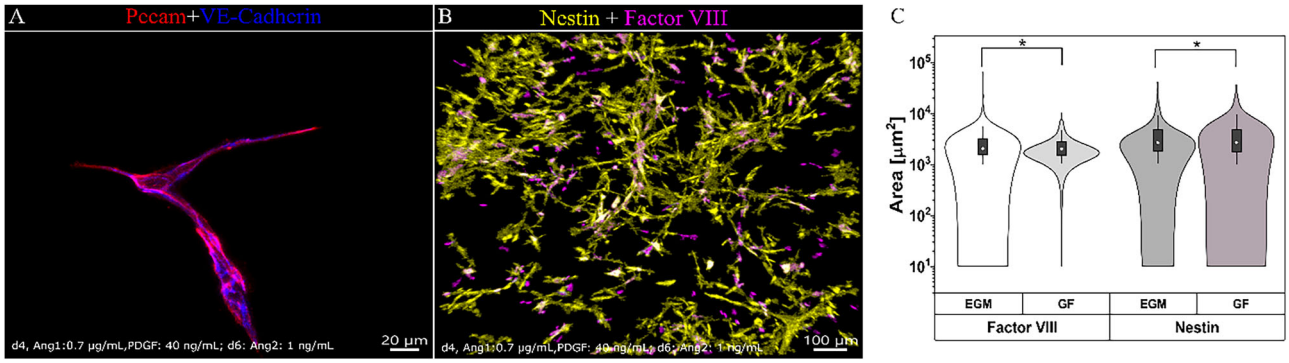

Figure 6. Endothelial characterization in 3NHDF:1HUVEC structures upon coculture in EGM-2 with the addition of the best GF combination. A) Immunofluorescence staining of PECAM/CD-31 (red) and VE-Cadherin (blue) analyzed after 7 days of culture. Scale bar: 20 µm. B,C) Immunofluorescence staining of nestin (yellow) and factor VIII (magenta), scale bar: 100 µm B) and their corresponding area C). The violin plots show the range between the first and third quarter indicated by the black bar in the violin and its standard deviation by the vertical line. The outliers and median are represented by the violin and the white dot. *n*: 3 replicates per condition ($p^* < 0.05$; $p^{**} < 0.01$; $p^{***} < 0.001$).

(Figure S5A–D, Supporting Information), we chose to magnetically align microgels with dimensions of 10 × 10 × 100 µm inside the surrounding PEG gel, modified with fibronectin, as vascular-like structure formation is the highest in these Anisogels. The forming blood vessel structures are oriented in the direction of the microgels, while the GF cocktail supported their formation and growth. Compared to EGM-2 without the addition of the GFs, the area, volume, and length are significantly higher when GFs are added. The GFs also have a positive effect on the number of structures, as there are significantly more with larger volumes. Of interest is also the number of branching points. In EGM-2, the structures have around 5 branching points, while with GFs, they have at least 10. However, this is much lower compared to the isotropic PEG hydrogels shown above (130). In addition, the vessels inside the Anisogels have less area, volume, and length, likely due to the steric hindrance caused by the microgels. Therefore, the number of microgels and their dimensions need to be further optimized to achieve aligned blood vessel structures inside Anisogels, without inhibiting their growth. In the case of primary neurons, grown inside the Anisogel, microgels with a width of 2.5 µm and length of 25 or 50 µm resulted in significantly more neurite extension compared with 5 × 5 × 50 µm microgels, even though both induced alignment.[64] Thus, thinner microgels at lower concentrations may be more optimal and will be further tested in the following studies. By aligning the vessels, it would be possible to create a predefined vascular network that would mimic the structure of native tissues. This may permit directing the network to reach and connect to specific targets in vitro, such as media inlets/outlets, to achieve improved dynamic flow systems. Such guided structures could potentially improve the development of specific tissue models, such as those targeting neuromuscular interactions.

2.8. Comparison with other Supporting Cells

We further asked whether our optimal GF mix also promotes the growth of more arterioles-like structures, using HUVECs in combination with other supporting cell types. Here, we tested the influence of pericytes and MSCs as supporting cells on vascular structure formation in the presence of the optimal GF cocktail and using the cell ratios and densities that were previously determined for NHDFs (**Figure 8**). In the case of the pericytes, no significant differences between the presence and absence of GFs could be observed in any of the investigated parameters, while structure formation is overall reduced compared to the counterpart conditions with fibroblasts and HUVECs as coculture. This indicates that the cell ratios and densities are not ideal for this condition. Still, the improved structure characteristics, such as number of branching points in GF conditions, suggest that GFs could also have a positive effect on vessel formation with pericytes, which will be investigated in the future with optimized cell ratios and densities.

In the case of MSCs, the addition of the optimal GF cocktail improves vessel formation as indicated by increased volume (2.1×10^5 µm³ to 1.5×10^5 µm³) and branching points (225–70) compared to controls. PDGF-BB is known to promote MSC proliferation,[85] while Ang1 has a protective effect against serum deprivation and is crucial for MSCs survival.[86] This makes our optimal GF cocktail suitable for systems that use MSCs as supporting cells, especially as MSCs do not produce enough Ang1 alone to promote angiogenesis.[87] In comparison to NHDFs as surrounding cells, the parameter values for MSCs are partly higher, especially the branching points (225–130), which makes them a suitable alternative for further work. Also, a combination of these two surrounding cell types could be tested.

2.9. Fibrosis Model

Finally, our vascular model is employed to test the induction of fibrosis. The same optimal GF cocktail is used with the optimized cell ratio and density of NHDFs and HUVECs inside isotropic PEG hydrogels modified with fibronectin and compared to EGM-2 without these GFs. To trigger fibrosis, 10 ng mL^{-1} TGF-β[47] is added to both cultures on d7 for 4 consecutive days, while analysis is performed on day 11. Due to the addition of TGF-β, fibroblasts seem to detach from previously formed vessels in GF conditions (**Figure 9**A,B white arrows), resulting in loss of structures as indicated by decreased volume, area, and the number of

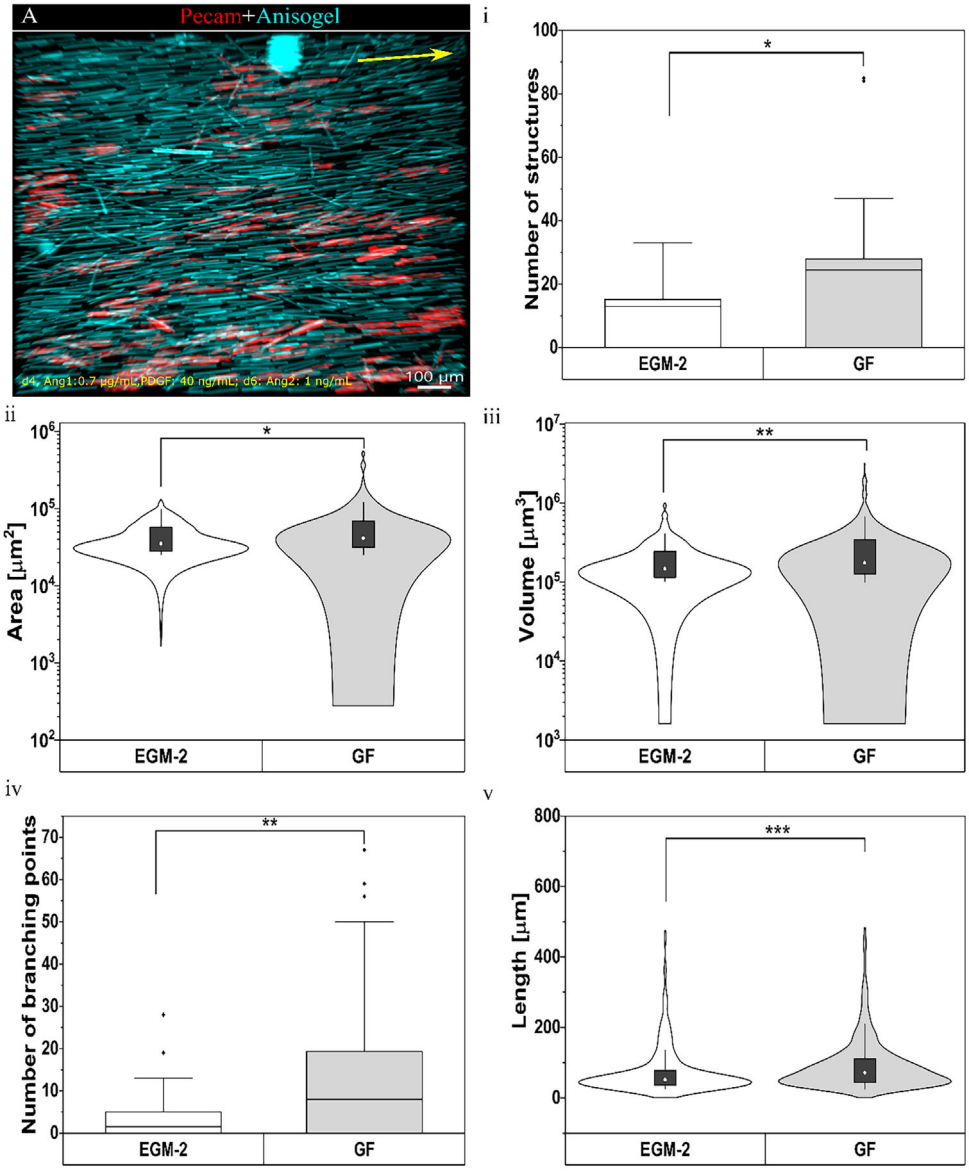

Figure 7. A) Alignment of vessel structures formed by HUVEC-fibroblast cocultures inside Anisogels. Immunofluorescence staining of PECAM/CD-31 structure (red) and 10 × 10 × 100 µm Anisogels (labeled with methacryloxyethyl thiocarbamoyl rhodamine B) cyan) in absence (EGM-2) and presence of the best GF combination analyzed after 7 days of culture, scale bar: 100 µm. Analysis of the corresponding number of structures (i), area (ii), volume (iii), branching points (iv), and length (v). The yellow arrow indicates the direction of the applied magnetic field to align the microgels. Bar graphs show the range between the first and third quarter indicated by the bar. The outliers and the mean value are represented by the error bars and the horizontal line, respectively. The violin plots show the range between the first and third quarter indicated by the black bar in the violin and its standard deviation by the vertical line. The outliers and median are represented by the violin and the white dot. *n*: 6 replicates per condition ($p^* < 0.05$; $p^{**} < 0.01$; $p^{***} < 0.001$).

branching points (Figure 9). In contrast, when TGF-β is added to the cells cultured in EGM-2 only, there is no significant decrease in these parameters. This may be explained by the fact that the structures are longer with a higher area and volume in the presence of GFs before TGF-β is added, which subsequently degenerate as TGF-β is added. This is also visible in an increased, yet not significant, number of structures after the addition of TGF-β. In addition, PDGF-BB and TGF-β have previously been shown to strengthen the signaling pathway-mediated activation of fibrosis-related proteins.[88] Ang1, on the other hand, which is essential for vessel integrity maintenance and supports fibroblast recruitment to the vessels, is inhibited by TGF-β.[44] In addition, collagen I secretion is significantly higher for the vessels treated with GF and TGF-β, compared to the vessels where no TGF-β is added (Figure 9 vi). In addition, the increase of collagen I (pixel area normalized to actin area) production due to TGF- β addition is significantly higher for the cells first grown with our optimal GF mixture, compared to cells grown in EGM-2. This fits the excessive collagen production by fibroblasts during fibrosis.[89]

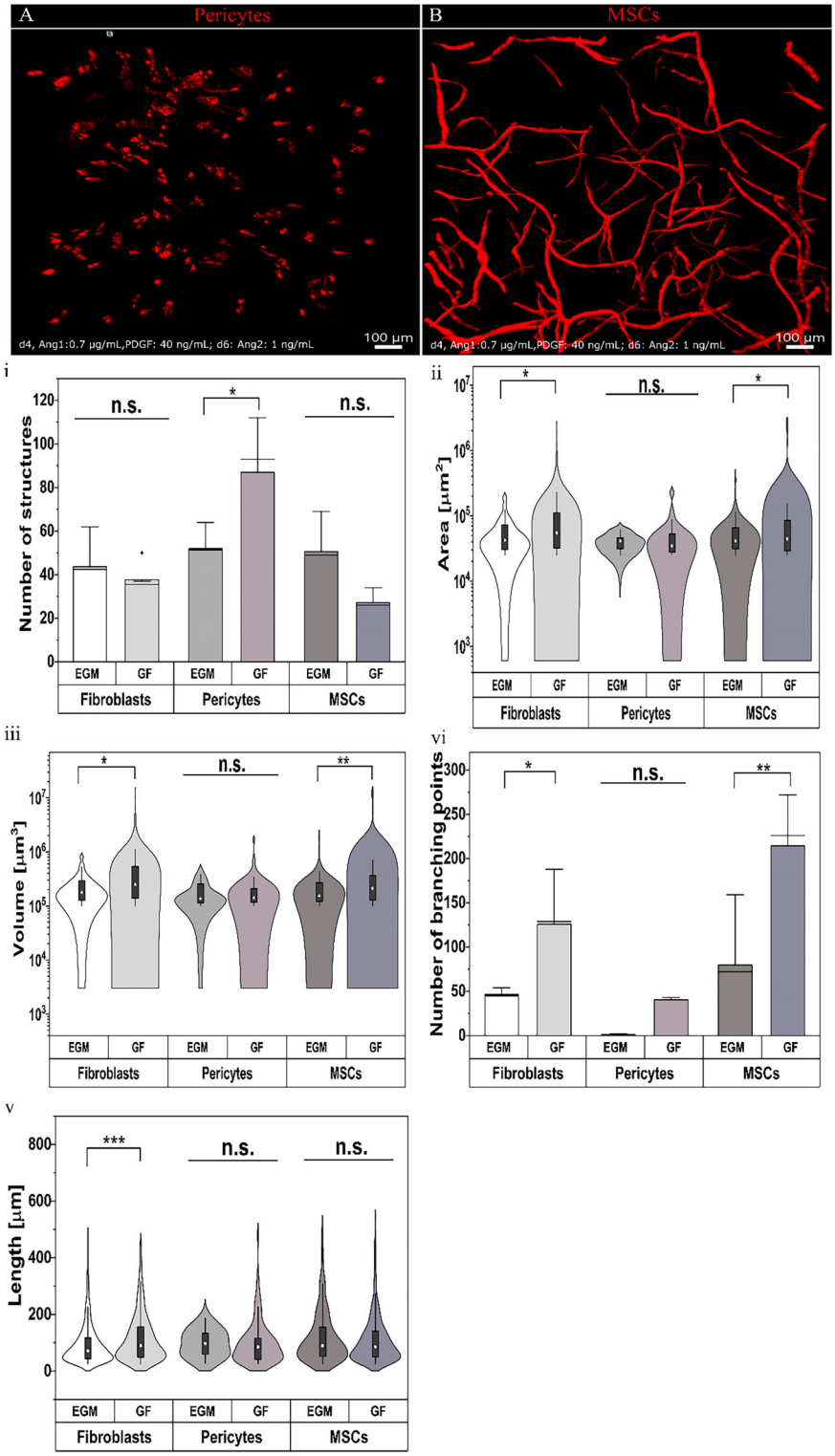

Figure 8. Comparison of different supporting cells. Immunofluorescence staining for PECAM/CD-31 (red) of the vascular structures inside the hydrogel in the absence (EGM-2) or presence of the optimal GF combination and using different supporting cell types: pericytes A) or MSCs B) analyzed after 7 days of culture, scale bar: 100 µm. Analysis of the corresponding number of structures (i), area (ii), volume (iii), branching points (iv), and length (v). Bar graphs show the range between the first and third quarter indicated by the bar. The outliers and the mean value are represented by the error bars and the horizontal line, respectively. The violin plots show the range between the first and third quarter indicated by the black bar in the violin and its standard deviation by the vertical line. The outliers and median are represented by the violin and the white dot. *n*: 3–6 replicates per condition ($p^* < 0.05$; $p^{**} < 0.01$; $p^{***} < 0.001$).

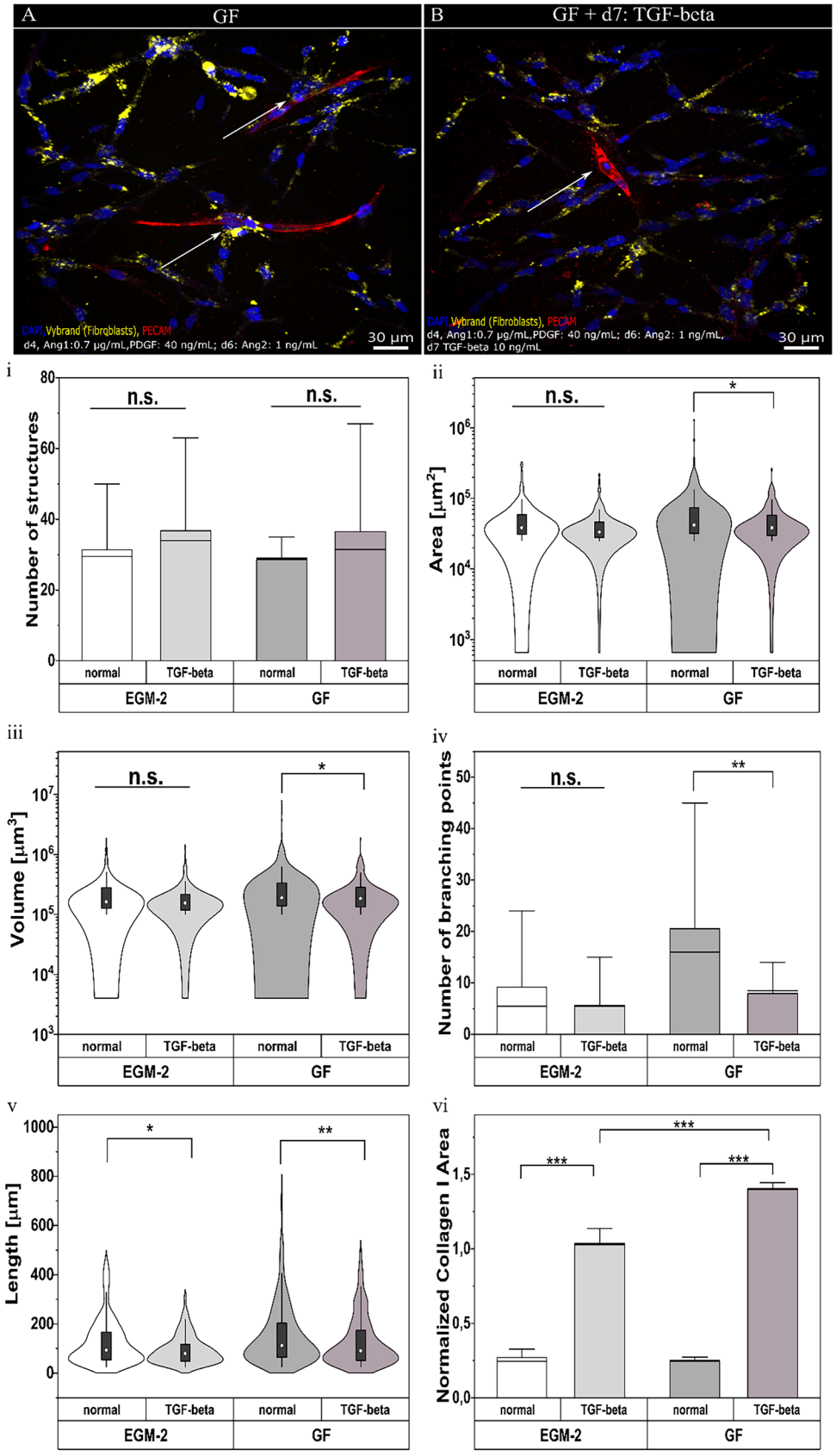

Overall, the addition of TGF-β induces fibrosis and is more effective in doing so in the presence of GFs. Therefore, these types of 3D vascular cultures are a good starting point to study fibrosis in vitro, and to test potential therapeutic approaches.

3. Conclusion and Outlook

Most GFs have a positive effect on vascularization in 3D co-cultures in PEG-based hydrogels modified with fibronectin. Already the addition of single GFs in basal medium or endothelial medium can increase the size of the vascular structures, with larger structures in the presence of endothelial medium. However, similar to the in vivo situation in the body, a combination of different GFs is needed at specific time points to achieve larger and more complex vascular structures. Here, we define an optimal GF cocktail, consisting of Ang1, PDGF-BB, and Ang2 in EGM-2 for in vitro studies. Both fibroblasts and MSCs support the formation of vessel-like structures with HUVECs under these culture conditions, with the MSCs leading to significantly more branching points. When cultured inside an Anisogel, vessel alignment is observed but the microgel parameters must be further optimized to not disrupt vessel formation. Finally, we demonstrated that this 3D culture can be employed to induce and study fibrosis in vitro. For further work and to use our optimal growth factor combination (Ang1+PDGF/Ang2 in EGM-2) in vivo, a drug delivery system will be developed that enables release at different time points. Also, due to the ongoing debate about HUVECs and their maturity, as they have site-specific phenotypes from the umbilical cord, or are described as fully differentiated, other sources of endothelial cells will be tested, such as blood outgrowth endothelial cells (BOEC), cord blood derived endothelial cells, or induced pluripotent stem cell (iPSC)-derived endothelial cells. In the case of BOECs or iPSC-derived ECs, this would enable us to have less premature cells and allow for the generation of patient-specific models.

4. Experimental Section

Cell culture: HUVECs (passage 1–5, pooled donors, Lonza) are cultured in tissue culture flasks in endothelial growth medium (EGM-2 ready-to-use kit, Promocell) supplemented with FBS (2%), epidermal growth factor (recombinant human, 5 ng mL^{-1}), basic fibroblast growth factor (recombinant human, 10 ng mL^{-1}), insulin-like growth factor (Long R3 IGF, 20 ng mL^{-1}), vascular endothelial growth factor 165 (recombinant human, 0.5 ng mL^{-1}), ascorbic acid (1 µg mL^{-1}), heparin (22.5 µg mL^{-1}), and hydrocortisone (0.2 µg mL^{-1}). Normal human dermal fibroblasts (NHDFs, passage 1–8, Promocell) are cultured in tissue culture flasks in DMEM (Gibco) supplemented with 10% FBS (Biowest or Gibco), 1% Antibiotics antimycotic solution (AMB, Gibco). Human bone marrow-derived mesenchymal stem cells (MSCs, passage 6, Lonza) were kindly provided by Dr. B. Spee and are cultured in tissue culture flasks in MSCGM mesenchymal stem cell growth medium (Lonza). Human placenta-derived primary pericytes (passage 4, PromoCell) are cultured in tissue culture flasks in pericyte growth medium 2 (PromoCell).

Table 2. Concentrations of growth factors tested.

Growth factor	Concentrations tested	Days
Ang1	0.2–2 µg mL^{-1}	Day 3–5
Ephrin-B2	0.3–2 µg mL^{-1}	Day 3–5
PDGF-BB	2–40 ng mL^{-1}	Day 4–6
Ang2	0.5–5 ng mL^{-1}	Day 5–6

The growth factors angiopoietin-1 (Ang-1, Promocell), Ephrin-B2 (Ephr, Abcam), platelet-derived growth factor-BB (PDGF-BB, Promocell), angiopoietin-2 (Ang-2, Promocell) are added on specific days (day 3–6) and concentrations as described in Table 1. The used concentrations are oriented from the literature for Ang1,[41,70] for Ephrin-B2,[32,71] for PDGF-BB,[40,68,72] and for Ang2.[73,74]

Hydrogel Preparation: The hydrogel was prepared as described previously.[60–65,90] In short, two separate batches of 8 arm star PEG-vinylsulfone (sPEG-VS, 20 kDa, Jenkem or Creative PEGWorks Technology) were conjugated with different peptide solutions in triethanolamine (pH = 8, Sigma-Aldrich): (H-NQEQVSPLERCG-NH2: Q-peptide, 1358.6 Da, Pepscan) or (Ac-FKGGGPQGIWGQERCG-NH2:c K-peptide, 1717.6 Da, Pepscan, or GenScript) using a Michael-type addition reaction via the thiol containing cysteine by incubating the solutions for 2 h at 37 °C. These solutions were dialyzed for 4 days in water at 4 °C to remove any unreacted peptides. Following this, the solutions were lyophilized, dissolved in water, sterilized, aliquoted, and stored at −20 °C until further use. For the gelation, the activated enzyme FXIII (CSL Behring GmbH, 1250 U FXIII) is needed. A 200 U mL^{-1} thrombin (Sigma-Aldrich) solution was diluted to 20 U mL^{-1} in an Ehrbar buffer (25 mM $CaCl_2$, 10 mM TRIS, 150 mM NaCl) and was incubated with the FXIII for 30 min at 37 °C, while shaking gently every 5 min. The FXIIIa was then aliquoted and stored at −80 °C until further use.

For making the gels, the two PEG conjugates were mixed in an equimolar ratio at a total concentration of 1–2 wt%, resulting in storage moduli between 10 and 1350 Pa, in EGM-2 or basal media with the 1000–4000 cells µL^{-1}, a 10X calcium buffer (0.1 M $CaCl_2$, 0.5 M Tris, 1.1 M NaCl), and fibronectin (1 µM, Sigma-Aldrich) or fibronectin fragment (5 µM, FNIII9*−10/12-14). Gelation was initiated by the addition of factor XIIIa. After mixing, the solution was pipetted in an 8 well ibidi slide chamber. The solution was crosslinked for 30 min at 37 °C and the chambers flipped back and forth four times to get a uniform distribution of cells. After the gelation was completed, cell media was added, and the samples were cultured for up to 7 days. Growth factors were added at specific time points and concentrations in EBM or EGM-2 media as indicated in **Table 2**.

Production of Microgels for the Anisogel: The microgels were prepared via the Print technique as described in the previous work.[60–64] In brief, a silicon wafer with a pattern in the required microgel dimension was filled with polydimethylsiloxane (PDMS, Sylgard 184, Sigma-Aldrich), mixed with its hardener 1:10, to create a mold. A polymer precursor solution out of PEG-DA (700 Da, Sigma-Aldrich), photoinitiator (Irgacure 2959, Sigma-Aldrich), diluent PEG-OH (200 Da, Sigma-Aldrich), methacryloxyethyl thiocarbamoyl rhodamine B (Polysciences), and SPIONs (EMG-700, Ferrotec) were spread over the PDMS mold. It was placed under UV light for 60 min

Figure 9. Fibrosis model. Immunofluorescence staining of PECAM/CD-31 (red), Vybrant staining of the fibroblasts (yellow), and Dapi (blue) of NHDF/HUVEC structures cultures in the absence or presence of the optimal GF combination in EGM-2 A), and after addition of TGF-β on d7 B) analyzed after 11 days of culture, scale bar: 30 µm, white arrows showing the NHDF/HUVEC contact; Quantification of structures: number of structures (i) with their area (ii), volume (iii), number of branching points (iv), and length (v); Normalized area of collagen I secretion (collagen I area divided by actin area) (vi). Bar graphs show the range between the first and third quarter indicated by the bar. The outliers and the mean value are represented by the error bars and the horizontal line, respectively. The violin plots show the range between the first and third quarter indicated by the black bar in the violin and its standard deviation by the vertical line. The outliers and median are represented by the violin and the white dot. *n*: 6 replicates per condition ($p^* < 0.05$; $p^{**} < 0.01$; $p^{***} < 0.001$).

under nitrogen. The mold was glued with a layer of 50% polyvinylpyrrolidone (360 kDa, Sigma-Aldrich) in water. After the glue dried, the mold was peeled off and the microgels were harvested. They were purified by washing with water and 70% Ethanol during UV sterilization. It was kept in PBS at 4 °C till use. The microgel suspension was counted in a Neubauer chamber and then washed again with the media used for cell culture.

To prepare the Anisogel samples, a calculated number of 10×10×100 µm microgels (1000 microgels μL^{-1})[65] or of microgels with other dimensions (Table S1, Supporting Information) was dispersed in a certain volume of EGM-2 together with the cells. The other components for the PEG-Q, K gel as mentioned before were added to the cell-microgel suspension. After mixing, FXIIIa was added, and the solution was pipetted in an ibidi chamber with magnets fitted around them.

Proliferation Assay (MTS Assay): For the MTS assay, around 20 000 cells were seeded in each hydrogel in a 24 well plate and cultivated for 1 or 3 days. The MTS working solution was prepared with cell culture media (1000 µL) and MTS reagent (200 µL). The growth media was removed and replaced with a MTS media solution. The sample was incubated in the dark for 2–4 h at 37 °C. 100 µL of the solution was added to a 96 well plate (3x for each well). Then, it was measured in a microplate reader *Synergy HT* from *BioTek* at 490 nm.

Fibrosis Model: Hydrogels containing the cells were grown in EGM-2 with or without the GF cocktail of 40 ng mL^{-1} PDGF-BB, 0.7 µg mL^{-1} Ang1, and 1 ng mL^{-1} Ang2 added at the time points as described in Table 1. On day 7, 10 ng mL^{-1}[47] of TGF-β (ACROBiosystems) was added and the hydrogels were cultured until day 11.

Immunochemical and Molecular Staining: After 7 days of culture (or 11 days for the fibrosis model), the media was removed and the hydrogel was washed for 30 min with PBS and subsequently fixed with 4% paraformaldehyde solution (AppliChem) for 1 h at room temperature. After washing the hydrogels twice with PBS for 30 min, the cells were permeabilized with 0.1% Triton X-100 (Sigma-Aldrich) in PBS for 20 min. After another washing step, the hydrogel culture was blocked with 4% bovine serum albumin (BSA, Seqens) in PBS for 4 h at room temperature. After removal of the blocking solution, the hydrogel was incubated with the primary antibody Pecam/CD31 (BioTechne, anti-mouse, 1:200 in 1% BSA+ 0.1% Triton X-100 in PBS) overnight at 4 °C. Excess antibody was removed by washing the samples 3 times for 30 min with PBS, followed by incubation with the secondary antibody (Alexa Fluor 555 goat anti-mouse; Invitrogen, 1:200) without or with Phalloidin iFluor 405 or 488 (Abcam, 1:1000) in PBS for 4 h at room temperature. The samples were washed again 3 times with PBS and DAPI (1:200) in PBS was added for 20 min. After washing again thrice, the samples were stored in PBS, in the dark at 4 °C until imaging. The same procedure was used for the other primaries VE-cadherin (Abcam, anti-rabbit, 1:200), nestin (Abcam, anti-mouse, 1:200), collagen I (Invitrogen, anti-rabbit 1:200), and factor VIII (Abcam, anti-rabbit, 1:200), and their corresponding secondaries Alexa Fluor 488, 633 goat anti-mouse (Invitrogen, 1:200), and Alexa Fluor 488 goat anti-rabbit (Invitrogen, 1:200). For the fibrosis model, NHDF were stained with Vybrant DiO (488, Thermo Fischer) solution.

Image Processing and Analysis: The samples were imaged using a Leica SP8 Tandem Confocal microscope using an air objective of 10×/0.3 N.A or a Perkin Elmer Opera Phenix Plus with a 10x/ N.A 0.3 air objective. Z-stacks of 200–250 µm thickness were acquired for each sample. These images were captured using the appropriate excitation wavelengths and the emission signals were captured using suitable detectors (hybrid detectors or photomultipliers) and detection sCMOS sensor cameras.

The obtained z-stack was converted to Imaris file format for evaluation. The data are evaluated with Imaris 9.9.0 software (Oxford instruments) by creating a 3D volume rendering of the Pecam stained structure using the surface module and the filament module to track the structures. The vascular structures were quantified according to their average surface area, volume, length, total number of vascular structures, and branching points. Bottom structures, which were not grown in 3D, were not considered. Structures with a total voxel number < 5000 were not counted; same with an area < 25 000 μm^2, volume < 100 000 μm^3, and length of < 25 µm as they were too small to be a vessel structure. For the normalization of the collagen I area, its area was evaluated as mentioned before, and was then divided by its corresponding actin area.

Statistical Analysis: Statistical data analysis was done in OriginPro 2022 using a one-way ANOVA with pair comparisons using Tukey's methods. The *p*-value below 0.05 was considered as a significant difference ($p^* < 0.05$; $p^{**} < 0.01$; $p^{***} < 0.001$).

Supporting Information

Supporting Information is available from the Wiley Online Library or from the author.

Acknowledgements

The authors gratefully acknowledged funding from the German Research Foundation (DFG) within the project LA 3606/3-1, the European Research Council within the ERC-2021-COG project 101043656, Heartbeat, and the European Union's Horizon 2020 research and innovation program under Grant Agreement No. 874586, project ORGANTRANS. The authors thank Nina Schöling for her contribution in preparing the microgels via PRINT. The authors thank Dr. B. Spee from Utrecht University for providing bone marrow-derived mesenchymal stem cells. This work was supported by the Core Facility "Two-Photon Imaging", a Core Facility of the Interdisciplinary Center for Clinical Research (IZKF) Aachen within the Faculty of Medicine at RWTH Aachen University.

Open access funding enabled and organized by Projekt DEAL.

Conflict of Interest

The authors declare no conflict of interest.

Data Availability Statement

The data that support the findings of this study are available from the corresponding author upon reasonable request.

Keywords

angiopoietin-1/-2, cell alignment, Ephrin-B2, platelet-derived growth factor-BB, vascular structures

Received: March 13, 2023
Revised: June 8, 2023
Published online: July 12, 2023

[1] J. D. Kakisis, C. D. Liapis, C. Breuer, B. E. Sumpio, *J. Vasc. Surg. Venous Lymphat. Disord.* **2005**, *41*, 349.
[2] L. A. Kunz-Schughart, J. A. Schroeder, M. Wondrak, F. van Rey, K. Lehle, F. Hofstaedter, D. N. Wheatley, *Am. J. Physiol.* **2006**, *290*, C1385.
[3] D. Gholobova, L. Decroix, V. Van Muylder, L. Desender, M. Gerard, G. Carpentier, H. Vandenburgh, L. Thorrez, *Tissue Eng., Part A* **2015**, *21*, 2548.
[4] D. Kolte, J. A. McClung, W. S. Aronow, *Vasculogenesis and Angiogenesis*, Elsevier Inc., Amsterdam **2016**.
[5] V. Mastrullo, W. Cathery, E. Velliou, P. Madeddu, P. Campagnolo, *Front. Bioeng. Biotechnol.* **2020**, *8*, 188.
[6] A. Banfi, G. von Degenfeld, H. M. Blau, *Curr. Atheroscler. Rep.* **2005**, *7*, 227.

[7] N. W. Gale, G. D. Yancopoulos, *Genes Dev.* **1999**, *13*, 1055.
[8] G. D. Yancopoulos, S. Davis, N. W. Gale, J. S. Rudge, S. J. Wiegand, J. Holash, *Nature* **2000**, *407*, 242.
[9] P. Carmeliet, *Nat. Med.* **2000**, *6*, 389.
[10] M. M. Martino, S. Brkic, E. Bovo, M. Burger, D. J. Schaefer, T. Wolff, L. Gürke, P. S. Briquez, H. M. Larsson, R. Gianni-Barrera, J. A. Hubbell, A. Banfi, *Front. Bioeng. Biotechnol.* **2015**, *3*, https://doi.org/10.1126/scitranslmed.3002614.
[11] H.-J. Lai, C.-H. Kuan, H.-C. Wu, J.-C. Tsai, T.-M. Chen, D.-J. Hsieh, T.-W. Wang, *Acta Biomater.* **2014**, *10*, 4156.
[12] J. K. Chae, I. Kim, S. T. Lim, M. J. Chung, W. H. Kim, H. G. Kim, J. K. Ko, G. Y. Koh, *Arterioscler. Thromb. Vasc. Biol.* **2000**, *20*, 2573.
[13] H. L. Xu, W. Z. Yu, C. T. Lu, X. K. Li, Y. Z. Zhao, *Biotechnol. J.* **2017**, *12*, https://doi.org/10.1002/biot.201600243.
[14] U. Fiedler, M. Scharpfenecker, S. Koidl, A. Hegen, V. Grunow, J. M. Schmidt, W. Kriz, G. Thurston, H. G. Augustin, *Blood* **2004**, *103*, 4150.
[15] C. Suri, J. McClain, G. Thurston, D. M. McDonald, H. Zhou, E. H. Oldmixon, T. N. Sato, G. D. Yancopoulos, *Science* **1998**, *282*, 468.
[16] N. Ferrara, *Am. J. Physiol.* **2001**, *280*, C1358.
[17] F. De Smet, B. Tembuyser, A. Lenard, F. Claes, J. Zhang, C. Michielsen, A. Van Schepdael, J. M. Herbert, F. Bono, M. Affolter, M. Dewerchin, P. Carmeliet, *Chem. Biol.* **2014**, *21*, 1310.
[18] M. Murakami, L. T. Nguyen, Z. W. Zhang, K. L. Moodie, P. Carmeliet, R. V. Stan, M. Simons, *J. Clin. Invest.* **2008**, *118*, 3355.
[19] J. Rouwkema, A. Khademhosseini, *Trends Biotechnol.* **2016**, *34*, 733.
[20] P. C. Maisonpierre, C. Suri, P. F. Jones, S. Bartunkova, S. J. Wiegand, C. Radziejewski, D. Compton, J. McClain, T. H. Aldrich, N. Papadopoulos, T. J. Daly, S. Davis, T. N. Sato, G. D. Yancopoulos, *Science* **1997**, *277*, 55.
[21] T. Sakurai, M. Kudo, *Oncology* **2011**, *81*, 24.
[22] J. Folkman, *Nat. Rev. Drug Discovery* **2007**, *6*, 273.
[23] H. K. Awada, N. R. Johnson, Y. Wang, *J. Controlled Release* **2015**, *207*, 7.
[24] P. C. Maisonpierre, C. Suri, P. F. Jones, S. Bartunkova, S. J. Wiegand, C. Radziejewski, D. Compton, J. McClain, T. H. Aldrich, N. Papadopoulos, T. J. Daly, S. Davis, T. N. Sato, G. D. Yancopoulos, *Science* **1997**, *277*, 55.
[25] N. P. Fam, S. Verma, M. Kutryk, D. J. Stewart, *Circulation* **2003**, *108*, 2613.
[26] E. D. Phelps, D. L. Updike, E. C. Bullen, P. Grammas, E. W. Howard, *Am. J. Physiol.* **2006**, *290*, C352.
[27] M. Ramsauer, P. A. D'Amore, *J. Clin. Invest.* **2002**, *110*, 1615.
[28] U. Fiedler, H. G. Augustin, *Trends Immunol.* **2006**, *27*, 552.
[29] H. U. Wang, Z. F. Chen, D. J. Anderson, *Cell* **1998**, *93*, 741.
[30] O. Salvucci, G. Tosato, *Adv. Cancer Res.* **2012**, *114*, 21.
[31] Y. Wang, M. Nakayama, M. E. Pitulescu, T. S. Schmidt, M. L. Bochenek, A. Sakakibara, S. Adams, A. Davy, U. Deutsch, U. Lüthi, A. Barberis, L. E. Benjamin, T. Mäkinen, C. D. Nobes, R. H. Adams, *Nature* **2010**, *465*, 483.
[32] H. Maekawa, Y. Oike, S. Kanda, Y. Ito, Y. Yamada, H. Kurihara, R. Nagai, T. Suda, *Arterioscler. Thromb. Vasc. Biol.* **2003**, *23*, 2008.
[33] S. Sawamiphak, S. Seidel, C. L. Essmann, G. A. Wilkinson, M. E. Pitulescu, T. Acker, A. Acker-Palmer, *Nature* **2010**, *465*, 487.
[34] D. Vreeken, H. Zhang, A. J. van Zonneveld, J. M. van Gils, *Int. J. Mol. Sci.* **2020**, *21*, 5623.
[35] S. Kuijper, C. J. Turner, R. H. Adams, *Trends Cardiovasc. Med.* **2007**, *17*, 145.
[36] Y. Xue, S. Lim, Y. Yang, Z. Wang, L. D. E. Jensen, E. M. Hedlund, P. Andersson, M. Sasahara, O. Larsson, D. Galter, R. Cao, K. Hosaka, Y. Cao, *Nat. Med.* **2011**, *18*, 100.
[37] M. Raica, A. M. Cimpean, *Pharmaceuticals* **2010**, *3*, 572.
[38] C. Rolny, I. Nilsson, P. Magnusson, A. Armulik, L. Jakobsson, P. Wentzel, P. Lindblom, J. Norlin, C. Betsholtz, R. Heuchel, M. Welsh, L. Claesson-Welsh, *Blood* **2006**, *108*, 1877.
[39] M. Uutela, M. Wirzenius, K. Paavonen, I. Rajantie, Y. He, T. Karpanen, M. Lohela, H. Wiig, P. Salven, K. Pajusola, U. Eriksson, K. Alitalo, *Blood* **2004**, *104*, 3198.
[40] R. J. F. C. do Amaral, B. Cavanagh, F. J. O'Brien, C. J. Kearney, *J. Tissue Eng. Regener. Med.* **2019**, *13*, 261.
[41] Y. Shin, J. S. Jeon, S. Han, G. S. Jung, S. Shin, S. H. Lee, R. Sudo, R. D. Kamm, S. Chung, *Lab Chip* **2011**, *11*, 2175.
[42] Y. Brudno, A. B. Ennett-Shepard, R. R. Chen, M. Aizenberg, D. J. Mooney, *Biomaterials* **2013**, *34*, 9201.
[43] M. Ruiz-Ortega, J. Rodríguez-Vita, E. Sanchez-Lopez, G. Carvajal, J. Egido, *Cardiovasc. Res.* **2007**, *74*, 196.
[44] J. Y. F. Chung, M. K. K. Chan, J. S. F. Li, A. S. W. Chan, P. C. T. Tang, K. T. Leung, K. F. To, H. Y. Lan, P. M. K. Tang, *Int. J. Mol. Sci.* **2021**, *22*, 7575.
[45] G. Untergasser, R. Gander, C. Lilg, G. Lepperdinger, E. Plas, P. Berger, *Mech. Ageing Dev.* **2005**, *126*, 59.
[46] B. C. Berk, *Physiol. Rev.* **2001**, *81*, 999.
[47] R. Kramann, R. K. Schneider, D. P. Dirocco, F. Machado, S. Fleig, P. A. Bondzie, J. M. Henderson, B. L. Ebert, B. D. Humphreys, *Cell Stem Cell* **2015**, *16*, 51.
[48] K. Wang, Q. Zhang, L. Zhao, Y. Pan, T. Wang, D. Zhi, S. Ma, P. Zhang, T. Zhao, S. Zhang, W. Li, M. Zhu, Y. Zhu, J. Zhang, M. Qiao, D. Kong, *ACS Appl. Mater. Interfaces* **2017**, *9*, 11415.
[49] Y. Zhang, K. Xu, D. Zhi, M. Qian, K. Liu, Q. Shuai, Z. Qin, J. Xie, K. Wang, J. Yang, *Adv. Fiber Mater.* **2022**, *4*, 1685.
[50] Y. Chen, X. Dong, M. Shafiq, G. Myles, N. Radacsi, X. Mo, *Adv. Fiber Mater.* **2022**, *4*, 959.
[51] M. V. Giraudo, D. Di Francesco, M. C. Catoira, D. Cotella, L. Fusaro, F. Boccafoschi, *Biomedicines* **2020**, *8*, 436.
[52] V. W. M. Van Hinsbergh, A. Collen, P. Koolwijk, *Ann. N. Y. Acad. Sci.* **2001**, *936*, 426.
[53] A. Lesman, J. Koffler, R. Atlas, Y. J. Blinder, Z. Kam, S. Levenberg, *Biomaterials* **2011**, *32*, 7856.
[54] Z. Wei, E. Volkova, M. R. Blatchley, S. Gerecht, *Adv. Drug Delivery Rev.* **2019**, *149–150*, 95.
[55] A. H. Zisch, U. Schenk, J. C. Schense, S. E. Sakiyama-Elbert, J. A. Hubbell, *J. Controlled Release* **2001**, *72*, 101.
[56] A. Zieris, S. Prokoph, K. R. Levental, P. B. Welzel, M. Grimmer, U. Freudenberg, C. Werner, *Biomaterials* **2010**, *31*, 7985.
[57] M. M. Martino, F. Tortelli, M. Mochizuki, S. Traub, D. Ben-David, G. A. Kuhn, R. Müller, E. Livne, S. A. Eming, J. A. Hubbell, *Sci. Transl. Med.* **2011**, *3*, 100ra89.
[58] M. M. Martino, P. S. Briquez, A. Ranga, M. P. Lutolf, J. A. Hubbell, *Proc. Natl. Acad. Sci. USA* **2013**, *110*, 4563.
[59] J. C. Rose, L. De Laporte, *Adv. Healthcare Mater.* **2018**, *7*, 1701067.
[60] J. C. Rose, M. Cámara-Torres, K. Rahimi, J. Köhler, M. Möller, L. De Laporte, *Nano Lett.* **2017**, *17*, 3782.
[61] J. C. Rose, M. Fölster, L. Kivilip, J. L. Gerardo-Nava, E. E. Jaekel, D. B. Gehlen, W. Rohlfs, L. De Laporte, *Polym. Chem.* **2020**, *11*, 496.
[62] J. C. Rose, D. B. Gehlen, A. Omidinia-Anarkoli, M. Fölster, T. Haraszti, E. E. Jaekel, L. De Laporte, J. C. Rose, D. B. Gehlen, A. Omidinia-Anarkoli, M. Fölster, T. Haraszti, E. E. Jaekel, L. De Laporte, *Adv. Healthcare Mater.* **2020**, *9*, 2000886.
[63] A. Omidinia-Anarkoli, S. Boesveld, U. Tuvshindorj, J. C. Rose, T. Haraszti, L. De Laporte, *Small* **2017**, *13*, 1702207.
[64] S. Babu, I. Chen, S. Vedaraman, J. Gerardo-Nava, C. Licht, Y. Kittel, T. Haraszti, J. Di Russo, L. De Laporte, *Adv. Funct. Mater.* **2022**, *32*, 2202468.
[65] C. Licht, J. C. Rose, A. O. Anarkoli, D. Blondel, M. Roccio, T. Haraszti, D. B. Gehlen, J. A. Hubbell, M. P. Lutolf, L. De Laporte, *Biomacromolecules* **2019**, *20*, 4075.
[66] Y. J. Blinder, A. Freiman, N. Raindel, D. J. Mooney, S. Levenberg, *Sci. Rep.* **2015**, *5*, 17840.

[67] X. Chen, A. S. Aledia, C. M. Ghajar, C. K. Griffith, A. J. Putnam, C. C. W. Hughes, S. C. George, *Tissue Eng., Part A* **2009**, *15*, 1363.
[68] S. Levenberg, J. Rouwkema, M. Macdonald, E. S. Garfein, D. S. Kohane, D. C. Darland, R. Marini, C. A. Van Blitterswijk, R. C. Mulligan, P. A. D'Amore, R. Langer, *Nat. Biotechnol.* **2005**, *23*, 879.
[69] P. Carmeliet, *Nat. Med.* **2000**, *6*, 389.
[70] T. I. Koblizek, C. Weiss, G. D. Yancopoulos, U. Deutsch, W. Risau, *Curr. Biol.* **1998**, *8*, 529.
[71] E. Groppa, S. Brkic, A. Uccelli, G. Wirth, P. Korpisalo-Pirinen, M. Filippova, B. Dasen, V. Sacchi, M. G. Muraro, M. Trani, S. Reginato, R. Gianni-Barrera, S. Ylä-Herttuala, A. Banfi, *EMBO Rep.* **2018**, *19*, https://doi.org/10.15252/embr.201745054.
[72] S. Lange, J. Heger, G. Euler, M. Wartenberg, H. M. Piper, H. Sauer, *Cardiovasc. Res.* **2009**, *81*, 159.
[73] I. Helfrich, L. Edler, A. Sucker, M. Thomas, S. Christian, D. Schadendorf, H. G. Augustin, *Clin. Cancer Res.* **2009**, *15*, 1384.
[74] G. Thurston, C. Daly, *Perspect. Med.* **2012**, *2*, https://doi.org/10.1101/cshperspect.a006650.
[75] A. V. Benest, A. H. Salmon, W. Wang, C. P. Glover, J. Uney, S. J. Harper, D. O. Bates, *Microcirculation* **2006**, *13*, 423.
[76] I. B. Lobov, P. C. Brooks, R. A. Lang, *Proc. Natl. Acad. Sci. USA* **2002**, *99*, 11205.
[77] J. Glade Bender, E. M. Cooney, J. J. Kandel, D. J. Yamashiro, *Drug Resist. Updat.* **2004**, *7*, 289.
[78] H. Xiao, Q. Huang, J. Q. Wang, Q. Q. Deng, W. P. Gu, *Neural Regener. Res.* **2016**, *11*, 735.
[79] M. M. Martino, P. S. Briquez, E. Güç, F. Tortelli, W. W. Kilarski, S. Metzger, J. J. Rice, G. A. Kuhn, R. Muller, M. A. Swartz, J. A. Hubbell, *Science* **2014**, *343*, 885.
[80] T. P. Richardson, M. C. Peters, A. B. Ennett, D. J. Mooney, *Nat. Biotechnol.* **2001**, *19*, 1029.
[81] I. Freeman, S. Cohen, *Biomaterials* **2009**, *30*, 2122.
[82] L. P. B. Guerzoni, J. Bohl, A. Jans, J. C. Rose, J. Koehler, A. J. C. Kuehne, L. De Laporte, *Biomater. Sci.* **2017**, *5*, 1549.
[83] D. Vestweber, *Arterioscler. Thromb. Vasc. Biol.* **2008**, *28*, 223.
[84] Y. Matsuda, M. Hagio, T. Ishiwata, *World J. Gastroenterol.* **2013**, *19*, 42.
[85] J. Zhang, F. Feng, Q. Wang, X. Zhu, H. Fu, L. Xu, K. Liu, X. Huang, X. Zhang, *Stem Cells Transl. Med.* **2016**, *5*, 1631.
[86] X. B. Liu, J. Jiang, C. Gui, X. Y. Hu, M. X. Xiang, J. A. Wang, *Acta Pharmacol. Sin.* **2008**, *29*, 815.
[87] Y. Li, L. Zheng, X. Xu, L. Song, Y. Li, W. Li, S. Zhang, F. Zhang, H. Jin, *Stem Cell Res Ther* **2013**, *4*, 113.
[88] X. Deng, K. Jin, Y. Li, W. Gu, M. Liu, L. Zhou, *Cell. Physiol. Biochem.* **2015**, *36*, 937.
[89] R. T. Kendall, C. A. Feghali-Bostwick, *Front. Pharmacol.* **2014**, *5*, 123.
[90] M. Ehrbar, S. C. Rizzi, R. G. Schoenmakers, J. A. Hubbell, F. E. Weber, M. P. Lutolf, *Biomacromolecules* **2007**, *8*, 3000.